Computational Quantum Chemical with Biological Studies on Uracil-5-Tertiary Sulfonamides

G. V. Gaurav [a] and K. Rama Krishna [b*]

[a] *Department of Chemistry, Gayatri Vidya Parishad College for Degree and PG Courses (A), Visakhapatnam, Andhra Pradesh, India.*
[b] *Department of Chemistry, Institute of science, GITAM (Deemed to be University), Visakhapatnam, Andhra Pradesh-530045, India.*

Authors' contributions

This work was carried out in collaboration between both authors. Both authors read and approved the final manuscript.

Article Information

Original Research Article

ABSTRACT

Aims: To study Computational Quantum Chemical (CQC), Pharmacokinetic and other biological components are listed in pairs of Uracil-5-Tertiary Sulfonamides "5-(4-(2,3-dihydrobenzo [b] [1,4]dioxine-2-carbonyl)piperazin-1-yl)sulfonyl)pyrimidine-2,4(1H, 3H)-dione " (I) and "N-butyl-N-methyl-2,4-dioxo-1,2,3,4 -tetrahydropyrimidine-5-sulfonamide " (II).
Methodology: NMR (^{1}H, ^{13}C), FT-Raman, FT-IR, and UV-Vis spectral chemical data were calculated and reported. DFT values for both combinations (I and II) were calculated using B3LYP / 6-31 + G (d, p) and B3LYP / 6-311 + G (2d, p). NMR chemical modification was calculated using the independent atomic orbital measurement method (GIAO). UV-Vis display is also calculated using the same basic sets.
Conclusion: The limits of Hyperpolarizability, HOMO and LUMO are listed. Pharmacokinetic properties (ADMET), drug similarity, bioactivity school, logP, pKa calculated using Molinspiration, pkCSM, Swiss ADME, Chem Axon.

Keywords: CQC; pharmacokinetic; drug likeness; bioactivity score; molinspiration and chem axon software.

_____

*Corresponding author: E-mail: karipeddirk@gmail.com

1. INTRODUCTION

The number of physicochemical, thermodynamic and spectral properties measured in the first half of the last century is very limited. Correlation-based models (linear or quadratic) have been used by iC-Vogue to explain variation in physicochemical/ biochemical/ pharmaceutical activities for a subgroup of compounds whose molecular properties are one digit. This passive data aggregation is the initial step of chemoinformatics_bigdata. The core of protein sequences and data of bio-molecules in different species is found in the field of bioinformatics. Since the 1970s, the development of molecular descriptors has progressed rapidly, and the discipline has a niche in chemical data discovery research. The number of descriptions from the different categories combined exceeds five to six thousand. However, fragments/atoms, bonds, number of rings/MW/MR/logP, etc. is still widely used in research to explore huge libraries of compounds. Computing Chemobiopharmaco is an integrative discipline that favors the investigation of the potential for the molecular space of drugs that are ongoing and approved.

Although the success rates of QSAR models using molecular descriptors for large subsets are commendable, the method is not without its flaws. Fully explicit knowledge of the structural representation function is unthinkable, and approaches to large-scale modeling are constantly evolving. This leads to situations where even a molecular descriptor does not adequately describe the actual behavior of a compound (drugs, toxic molecules, etc.) in drug/material design.

Missing, correlated, and redundant (arithmetic similarity) information in the descriptor matrix for a set of molecules is truncated in the data preprocessing step. The quantitative variation of some descriptors (log P, solubility, etc.) is due to differences in the basic definitions and the number/type of compounds used in the parameterization of paradigm. PCA, PLASA and NN surpass the numerical correlation between descriptor columns in the classification/regression analysis.

Over the past two decades, advances in hardware (GPU, TPU), speed (peta/exa flops), memory (exa/peta bytes), and knowledge-based work (methods) have poured into the world. The pruning of very large numbers (10K to 1 million) compounds in the description space of 100 to 5K has spurred the development of reliable drugs.

Uracil derivatives in general and 5-Fluorouracil (5-FU) in particular are an anti-metabolite used in the treatment of gastric tract/breast/liver cancer [1]. The N1-substituted derivatives, nucleoside analog of 5- iodouracil and 5-trifluoromethyluracil show antiviral activity. [2] N1 N3-disubstituted uracils possesses antibacterial and antifungal activities.

The synthesis and characterization of "5-(4-(2,3-dihydrobenzo[b][1,4]dioxine-2-carbonyl) piperazin-1-yl) sulfonyl) pyrimidine-2,4(1H,3H)-dione" (I) and "N-butyl-N-methyl-2,4-dioxo-1,2,3,4-tetrahydropyrimidine-5-sulfonamide" (II) and their characterization as well as activity studies have been reported by Sasidhar [2]. In this paper the results of the Computational Quantum Chemical studies, Pharmacokinetic and other physicochemical properties have been discussed and compared with the experimental result of thesis submitted by Sasidhar.

2. MATERIALS AND METHODS

2.1 Computational Details

Gaussian 16 was used to do the DFT computations [3]. Geometric optimization of compounds was performed using the B3LYP exchange-correlation functional using the basis sets 6-31+G (d, p) and 6-311+G (2d, p). When the Gaussian 16 software package was used, the Gauss View 6 programme was used for visualization [4]. The theoretical NMR (^{1}H and ^{13}C) chemical shifts were determined using the GIAO method at the B3LYP/6-31+G (d, p) and B3LYP/6-311+G (2d, p) levels of theory, with DMSO serving as the standard reference. Theoretical absorption wavelengths, oscillator strengths (f), and main contributions to electronic transitions were computed in DMSO as solvent using TD-DFT CAM-B3LYP/6-311+G (2d, p) basis level (SMD model). Molinspiration [5,6], pkCSM [7], SwissADME [8,9], and Chemaxon [10] tools were used to investigate biological features such as absorption, distribution, metabolism, excretion, toxicity, physicochemical qualities, lipophilicity, pharmacokinetics, and drug resemblance.

3. RESULTS

3.1 Molecular Geometry

The optimal geometrical parameters for both compounds were calculated using the DFT/B3LYP 6-31+G (d, p) and DFT/B3LYP 6-

311+G (2d, p) levels of theory. Figs. 1 and 2 show the input and optimized geometries with atom labeling. This work includes computations in both the gas phase and the solvent phase. The results of DFT calculations on infrared, ^{1}H, and ^{13}C NMR have been compared to those found experimentally in the Sasidhar thesis [2].

Calculations of DFT were carried out using the Gaussian 16 package [3]. Optimization of geometrical compounds was carried out using B3LYP exchange functional correlation using the basis sets 6-31 + G (d, p), and 6-311 + G (2d, p). Gauss View 6 was designed to display situations involving the Gaussian 16 software suite. [4] Chemical mutations at the theoretical level of B3LYP / 6-31 + G (d, p) and B3LYP / 6-311 + G (2d, p) were obtained using the GIAO method, with DMSO serving as a standard reference. In DMSO as solvent, the TD-DFT CAM-B3LYP/6-311+G (2d,p) level base, theoretical absorption wavelengths, oscillator power (f), and key contributions to electronic conversion are presented (SMD model). Molinspiration [5,6], pkCSM [7], SwissADME [8,9], and ChemAxon [10] technologies are used to determine biological parameters such as absorption, distribution, metabolism, excretion, toxicity, physicochemical qualities, lipophilicity, pharmacokinetics, and drug resemblance.

4. DISCUSSION

Molecular Geometry: The geometric parameters for both chemicals are calculated by DFT/ B3LYP 6-31 + G (d, p), DFT/B3LYP 6-311 + G (2d, p) level of theory. Input and fine-tuned geometries have an atomic label shown in Figs. 1 and 2. In this work, calculations were performed on the gas and solvent phases. Infrared results, ^{1}H and ^{13}C NMR obtained in DFT calculations were compared with Sasidhar test results [2].

Vibrational assignments: The vibrational spectra obtained experimentally (FT-IR) were compared

to the theoretically received spectra. Compounds I and II contain 47 atoms and 220 electrons, 32 atoms and 138 electrons. The theoretical and actual FT-IR spectra of each molecule are given in Figs 3 and 4. Tables 1 and 2 contain experimental (FT-IR) observations, computed vibrational wave numbers (un-scaled and scaled), and complete key vibrational modes. Due to electron correlation results and inadequacy of the foundation set, the experimental wave numbers are typically smaller than the computed wave numbers. As a result, estimated wave numbers are scaled by a factor of 0.933. The predicted Raman intensities were calculated using the GAUSSIAN 16 software, and the numbers were tabulated. The resulting spectrum is shown in Figs 5 and 6.

N-H vibrations: The hetero-aromatic shape suggests the presence of N-H stretching vibration above 3200 cm^{-1}, that is the function area for prepared identity of this shape. These are the standard variety for CH_3, NH_2 and C-H vibrations. The N-H stretching vibration takes place with inside the area 3500-3200 cm^{-1}. For compound I the scaled N-H stretch turned into calculated at 3359 cm^{-1} with the aid of using B3LYP/6-31G (d,p) fueloline section, at 3331cm^{-1} with the aid of using B3LYP/6-31G+(d,p) solvent phase and 3319 cm^{-1} B3LYP/6-311G+(2d,p) solvent section, at 3346 cm^{-1} by B3LYP/ 6-311G+(2d,p) fueloline section and the experimental values discovered at 3280 cm^{-1} in FT-IR spectrum. The stretching vibration takes place with inside the area 3500-3200 cm^{-1}. For compound II the scaled N-H stretch turned into calculated at 3359 cm^{-1} with the aid of using B3LYP/6-31G(d,p) fueloline section, at 3334 cm^{-1} with the aid of using B3LYP/6-31G+(d,p) solvent section and 3322 cm^{-1} B3LYP/6-311G+(2d,p) solvent section, at 3347 cm^{-1} with the aid of using B3LYP/ 6-311G+(2d,p) fueloline section and the experimental values discovered at 3200 cm^{-1} in FT-IR spectrum.
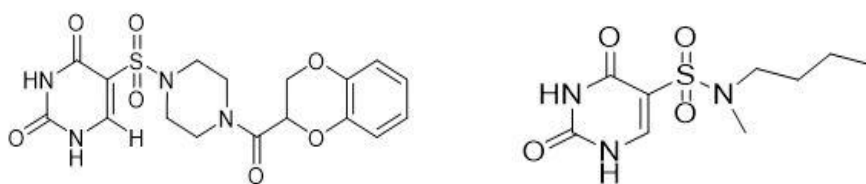
Fig. 1. Input structure of 5-(4-(2,3-dihydrobenzo[b][1,4]dioxine-2-carbonyl)piperazin-1-yl)sulfonyl)pyrimidine-2,4(1H,3H)-dione and N-butyl-N-methyl-2,4-dioxo-1,2,3,4-tetrahydro pyrimidine-5-sulfonamide
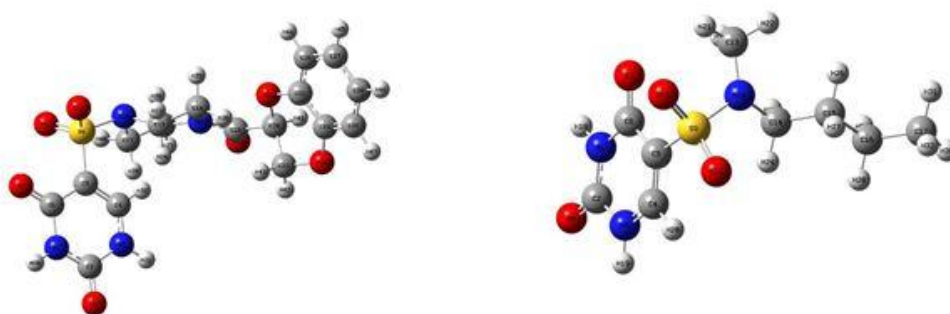
Fig. 2. The optimized geometrical structure of 5-(4-(2,3-dihydrobenzo[b][1,4]dioxine-2-carbonyl)piperazin-1-yl)sulfonyl)pyrimidine-2,4(1H,3H)-dione and N-butyl-N-methyl-2,4-dioxo-1,2,3,4-tetrahydropyrimidine-5-sulfonamidein solvent phase
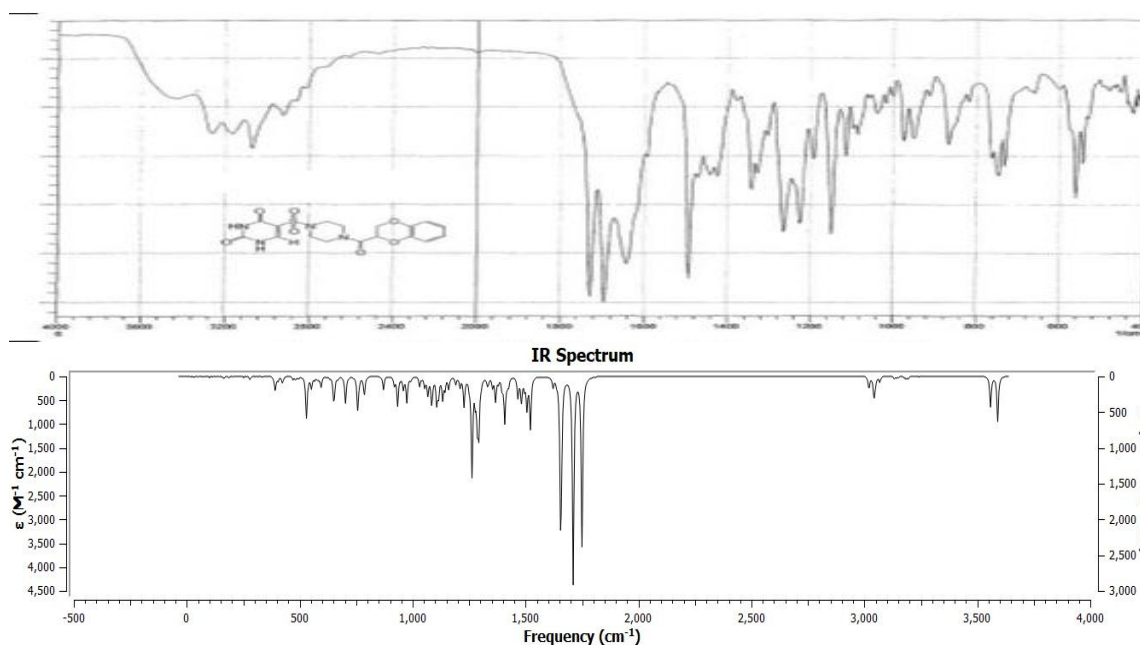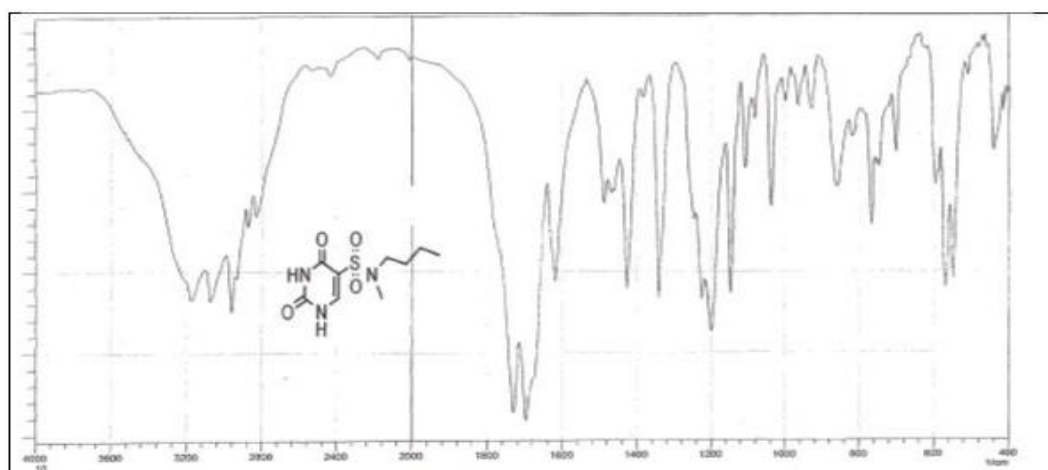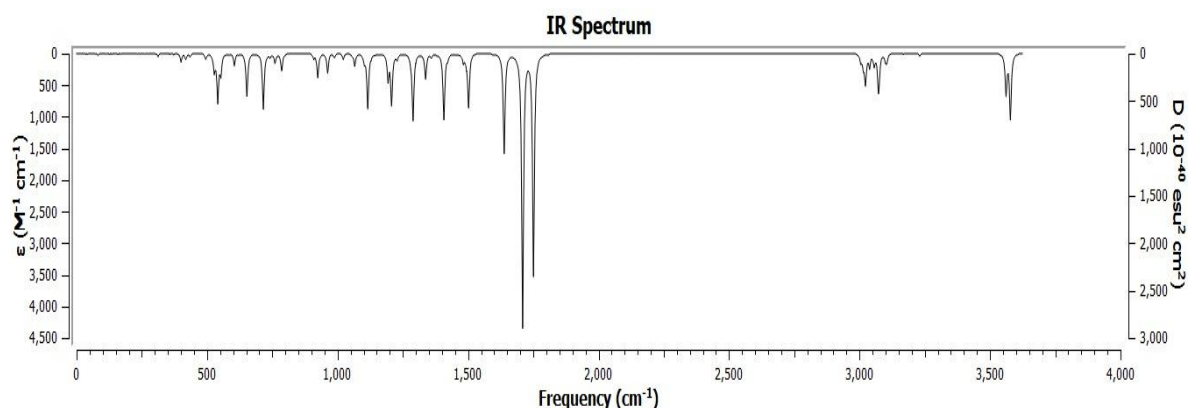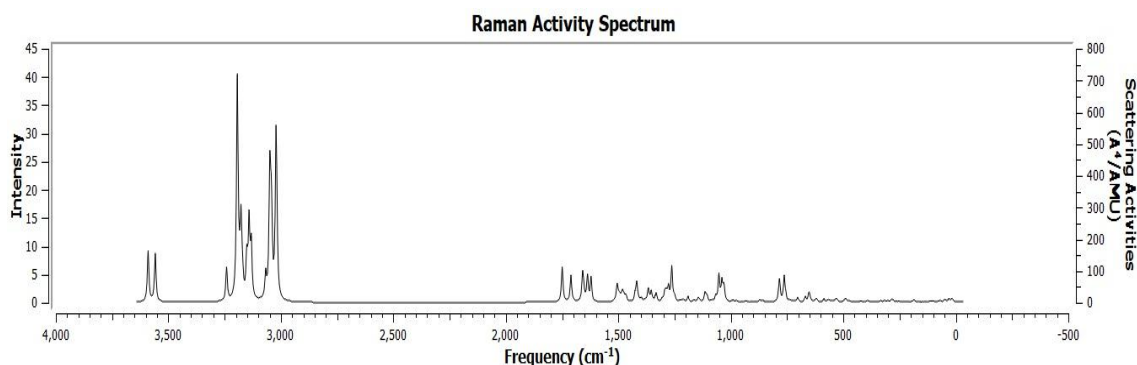

Fig. 3. Experimental and Theoretical FT-IR spectra of 5-(4-(2,3-dihydrobenzo[b][1,4]dioxine-2-carbonyl)piperazin-1-yl)sulfonyl)pyrimidine-2,4(1H,3H)-dione
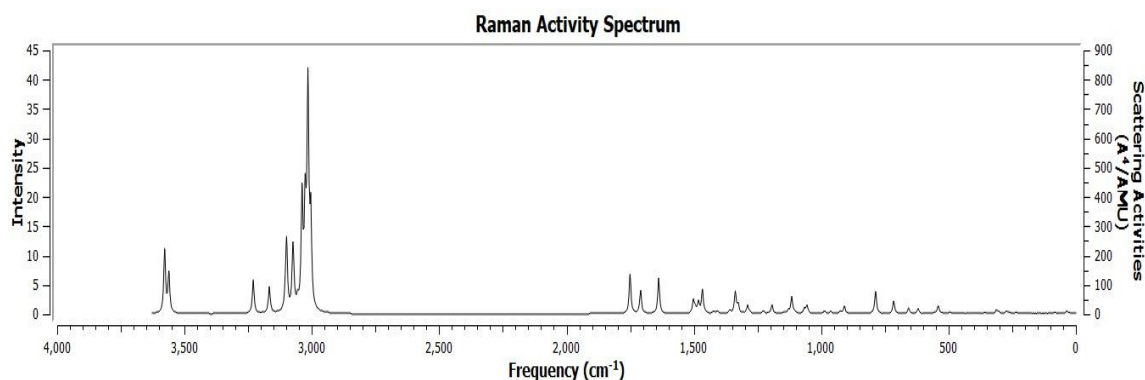
IR Spectrum

Fig. 4. Experimental and Theoretical FT-IR spectra of N-butyl-N-methyl-2, 4-dioxo-1, 2, 3, 4-tetrahydropyrimidine-5-sulfonamide

Raman Activity Spectrum

Fig. 5. Computational Raman spectra of 5-(4-(2,3-dihydrobenzo[b][1,4]dioxine-2-carbonyl)piperazin-1-yl)sulfonyl)pyrimidine-2,4(1H,3H)-dione

Raman Activity Spectrum

Fig. 6. Computational Raman spectra of N-butyl-N-methyl-2, 4-dioxo-1, 2, 3, 4-tetrahydropyrimidine-5-sulfonamide

The theoretically values with the aid of using B3LYP/6-31G (d,p) and B3LYP/6-311+G(2d,p) strategies display superb settlement with the recorded experimental values. C-H vibrations: In fragrant compounds, the C-H stretching wavenumbers seem with inside the variety 3100–3000 cm^{-1} that is the function area for the prepared identity of C-H stretching vibrations [11]. In this area, the bands have been now no longer affected notably with the aid of using the character of substituent.

The C-H stretching modes normally seem with sturdy Raman depth and are enormously polarized. The theoretically computed values for compound I at 3018 cm^{-1} with the aid of using

B3LYP/6-31G(d,p) fueloline section, at 3049 cm^{-1} with the aid of using B3LYP/6-31G+(d,p) solvent section, 3024 cm^{-1} with the aid of using B3LYP/6-311G+(2d,p) solvent section and at 2977 cm^{-1} with the aid of using B3LYP/ 6-311G+(2d,p) fueloline section and the experimental values discovered at 3180 cm^{-1}and for compound II the theoretically computed values at 2904 cm^{-1} with the aid of using B3LYP/6-31G(d,p) fueloline section, at 2915 cm^{-1} with the aid of using B3LYP/6-31G+(d,p) solvent section, 2896 cm^{-1} with the aid of using B3LYP/6-311G+(2d,p) solvent section. At 2887cm^{-1} with the aid of using B3LYP/ 6-311G+(2d,p) fueloline section and the experimental values discovered at 3100 cm^{-1} in FT-IR spectrum approach proven exact settlement with experimental observations.

C=O Vibrations: The C=O stretching vibrations is Raman and IR active. It is medium at 1600 cm^{-1} and really susceptible at 1111 cm^{-1} in IR. The computed values of compound I are discovered at 1695, 1649, 1632 and 1678 cm^{-1} respectively for B3LYP/6-31G(d,p) fueloline section, B3LYP/6-31G+(d,p) solvent section, B3LYP/6-311G+(2d,p) solvent section and B3LYP/ 6-311G+(2d,p) fueloline section at mode 117 and 1667, 1613, 1596 and 1651 cm^{-1} respectively for in B3LYP/6-31G(d,p) fueloline section, B3LYP/6-31G+(d,p) solvent section, B3LYP/6-311G+(2d,p) solvent section and B3LYP/ 6-311G+(2d,p) fueloline section at mode 116.

The experimental values for those modes are 1720 cm^{-1} and 1700 cm^{-1}, respectively. The computed values of compound II are discovered at 1693, 1651, 1633 and 1676 cm^{-1} respectively for B3LYP/6-31G(d,p) fueloline section, B3LYP/6-31G+(d,p) solvent section, B3LYP/6-311G+(2d,p) solvent section and B3LYP/ 6-311G+(2d,p) fueloline section at mode seventy five and 1651,1610,1594 and 1634 cm^{-1} respectively for B3LYP/6-31G(d,p) fueloline section, B3LYP/6-31G+(d,p) solvent section, B3LYP/6-311G+(2d,p) solvent section and B3LYP/ 6-311G+(2d,p) fueloline section at mode 74. The experimental values for those modes are 1720 and 1680 cm^{-1} respectively. This C=O vibration produces a big quantity without cost electrons and this area of the molecule is extra bioactive with the human proteins and acts as a drug.

C=C Vibrations: The C=C fragrant stretching vibration offers upward thrust to function bands in each the discovered FT-IR spectra, protecting the spectral variety from 1600-1400 cm^{-1} [12].

The theoretically computed an-harmonic frequencies at 1556 cm^{-1} with the aid of using B3LYP/6-31G(d,p) fueloline section, at 1554 cm^{-1} with the aid of using B3LYP/6-31G+(d,p) solvent section, 1543 cm^{-1} with the aid of using B3LYP/6-311G+(2d,p) solvent section and at 1551cm^{-1} with the aid of using B3LYP/ 6-311G+(2d,p) fueloline section approach and the C=C stretching vibrations for the compound II were discovered in FT-IR spectrum at 1440 cm^{-1} have been assigned to C=C stretching vibration. The theoretically computed an-harmonic frequencies at 1546 cm^{-1} with the aid of using B3LYP/6-31G(d,p) fueloline section, at 1533 cm^{-1} with the aid of using B3LYP/6-31G+(d,p) solvent section, 1528 cm^{-1} with the aid of using B3LYP/6-311G+(2d,p) solvent section and at 1541 cm^{-1} with the aid of using B3LYP/6-311G+(2d,p) fueloline section approach confirmed an awesome settlement with experimental data. Non Linear Optical Properties: Organic NLO substances are determined with inside the vanguard of contemporary studies in substances science. In those regards, the NLO houses of each the compounds have additionally been addressed with the aid of using the DFT calculations of polarizability and primary order hyper-polarizability (Parallel & Perpendicular), Energy and Dipole second.

The houses for the compounds I and II are expressed as electric dipole second, polarizability, and primary order hyper-polarizability (μ, α, Δ and β). NLO houses are found in atomic devices with Gaussian output (a.u). These are converted to conventional devices by using 1 a. u. = 8.63x10-30 esu for, 1 a. u. = 2.54 Debye for, and 1 a. u. = 0.15x10-24 esu for [13]. Table 3 summarises the general static dipole second (μ), implied polarizability (α), anisotropy of the polarizability (Δ), and implied first-order hyperpolarizability (β) of each compound.

Because, the urea molecule was considered to be a prototypical molecule in terms of the NLO houses, the computational consequences obtained were in comparison to the urea. To compare, NLO houses for the urea molecule were calculated on an equal stage of principle for each of the compounds. The calculated dipole second is 3.2 D, which is significantly less than the dipole second of urea, which is 3.89 D. Each compound's static polarizability and primary order hyper-polarizability are determined in esu devices to be 21.68 x 10-24 to 29.78 x 10-24 and 0.41 x 10-30 to 0.45 x 10-30, respectively. The

conclusion is that hyper-polarizability is approximately 0.75 times greater than that of urea (total= 0.62 x 10-30 esu).

Observations on NMR spectroscopy: Chemical shifts are frequently used to determine the shape of natural compounds. They are frequently used to determine the proper size of magnetic houses. The theoretical NMR chemical shifts for B3LYP/6-31G+(d,p) and B3LYP/6-311G+(2d,p) are determined using the GIAO method, with DMSO serving as a reference. Table 1-3 compares theoretical NMR (^{1}H and ^{13}C) spectra to experimental NMR (^{1}H and ^{13}C) spectra and chemical shifts. Carbon atoms within the fragrant ring have chemical shifts between 106-143 and 104-143 ppm in ^{13}C NMR. Carbon atoms are connected to oxygen atoms via a double bond in

the range of 134-143 parts per million [14, 15]. Chemical shift values of carbon atoms within the fragrant ring were discovered experimentally in the ranges 149-165 and 111-159 ppm for each of the compounds. These values are perfectly consistent with experimental results. At 143 and 150 ppm, the C2 atom is discovered to be connected to the oxygen atom via a double bond. Chemical shifts of fragrant protons are considered to be between 6.9-7.1 and 7.95 ppm. These chemical shifts in the Uracil protons of the hoop shape were discovered experimentally at 11.4 ppm, while they were theoretically discovered at 8.03 and 8.20 ppm. This conclusion is entirely consistent with the literature [16]. All calculated NMR chemical shift values (^{1}H, ^{13}C) are in perfect agreement with experimentally determined values.
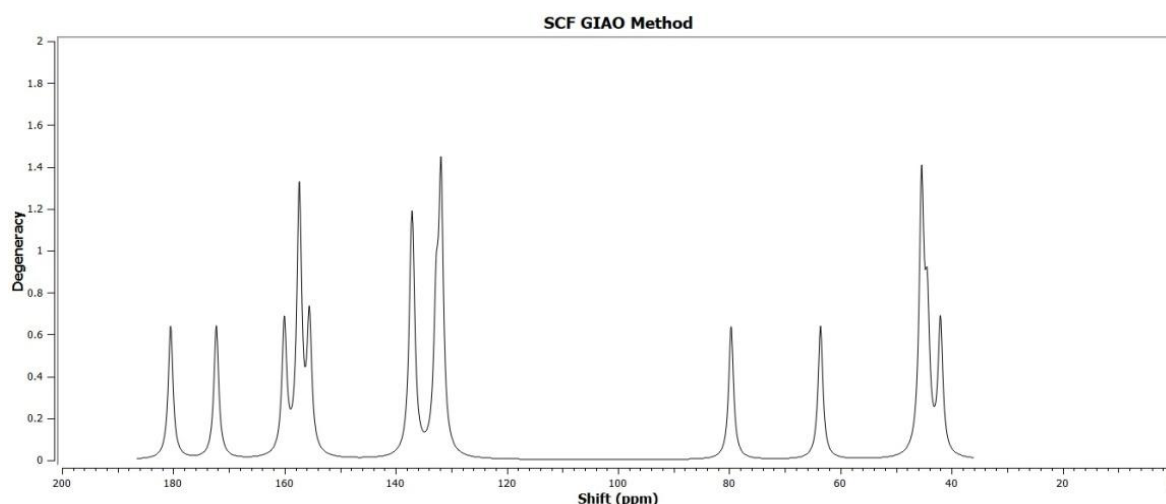

Fig. 7. Computational ^{13}CNMR spectra of 5-(4-(2,3-dihydrobenzo[b][1,4]dioxine-2-carbonyl)piperazin-1-yl)sulfonyl)pyrimidine-2,4(1H,3H)-dione
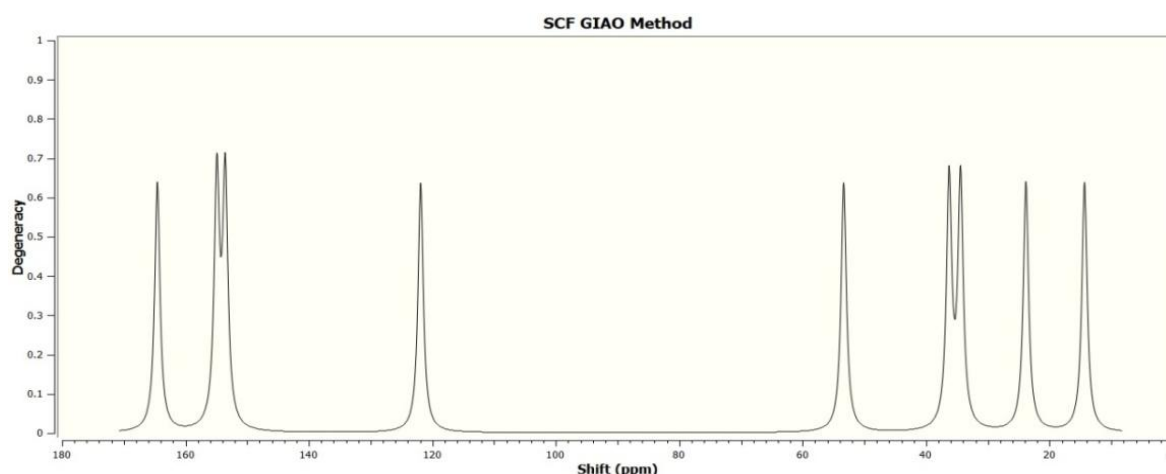
Fig. 8. Computational ^{13}CNMR spectra of N-butyl-N-methyl-2, 4-dioxo-1, 2, 3, 4-tetrahydropyrimidine-5-sulfonamide
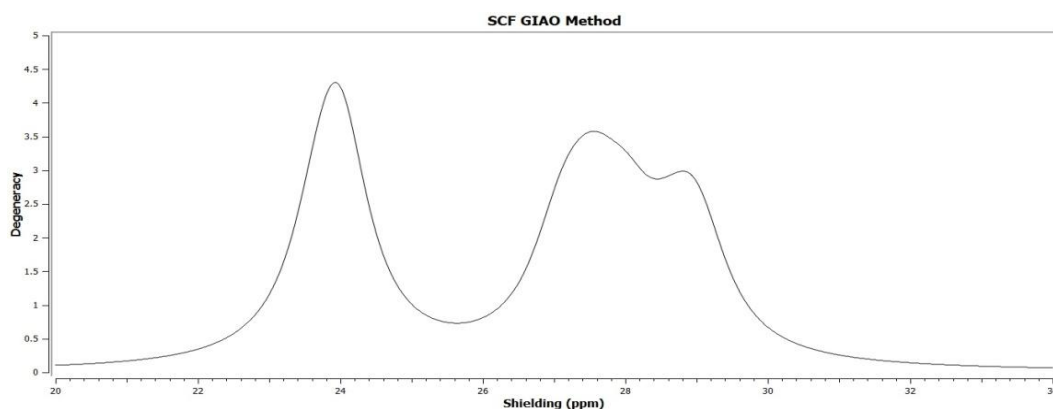
Fig. 9. Computational ^{1}H NMR spectra of 5-(4-(2,3-dihydrobenzo[b][1,4]dioxine-2-carbonyl)piperazin-1-yl)sulfonyl)pyrimidine-2,4(1H,3H)-dione
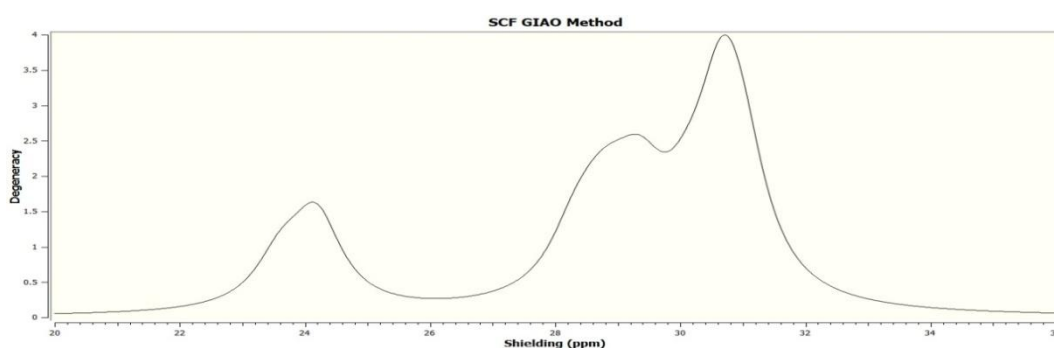
Fig. 10. Computational ^{1}H NMR spectra of N-butyl-N-methyl-2, 4-dioxo-1, 2, 3, 4-tetrahydropyrimidine-5-sulfonamide

UV – Visible Analysis: UV-vis inspection Time-Dependent DFT computations are the most advanced and widely used method for evaluating digital spectra of molecules. In this work, the transitions from the ground state to the excited state are typically described by a single electron excitation between molecular orbital's. This calculation yields the molecular geometry of the excited kingdom, the absorption maxima (max), the oscillator strengths (f), and the molecule's excitation strength [17]. The predicted UV-Vis spectra for DFT with B3LYP 6-31 G+ (d, p), B3LYP 6-311 G+ (d, p), and TD-DFT with B3LYP 6-311 G+ (d, p) foundation degrees in DMSO as solvent (SMD model) are shown in Figs 11 and 12.

4.1 Frontier Molecular Orbital (FMO) Studies

The energies and distributions of the FMO are extremely advantageous indicators of reactivity. The HOMO and LUMO molecular orbital's are the frontier molecular orbital's. The HOMO symbol denotes the ability to donate an electron, whereas the LUMO symbol denotes the ability to gain an electron [18]. The energy gap between the HOMO and LUMO orbital's is a critical parameter in determining and understanding molecular transport properties. HOMO-LUMO and (H-1) - (L+1) plots for compound I are shown in Fig. 13. EHOMO = -0.224 eV and ELUMO = -0.057 eV are the HOMO and LUMO energies, respectively, and the power hole is found to be 0.167 eV for compound I. HOMO = -0.248 eV and ELUMO = -0.058 eV are the energies of HOMO and LUMO, respectively, while the power hole is discovered to be 0.189 eV. The energy hole is regarded as a reactivity indicator, and because the price of the energy hole is less than 1 eV, each of the compounds may be considered fairly solid molecules.

4.2 pk CSM

It is a machine learning tool to predict the pharmacokinetic properties (ADMET) are calculated by using "pkCSM" of molecules. These parameters have been calculated and are summarized in Table 1.
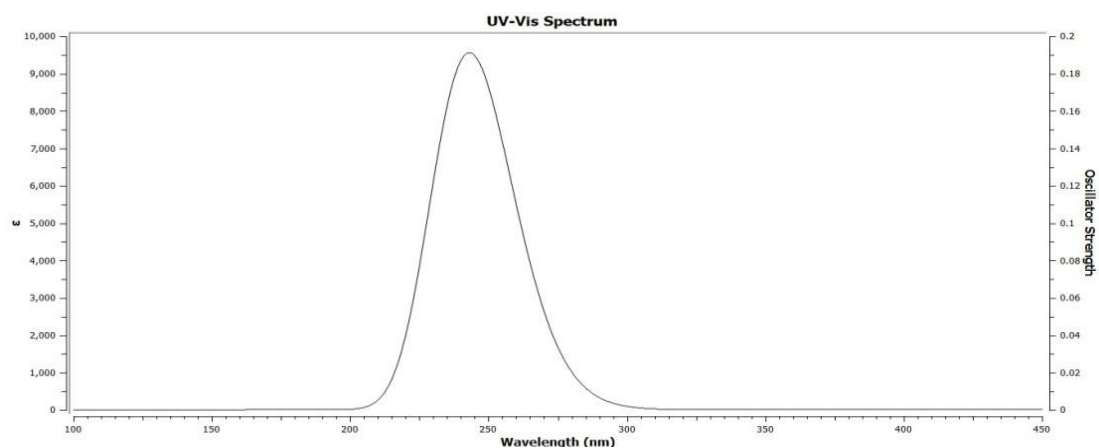
Fig. 11. Computational UV-Vis spectra of 5-(4-(2,3-dihydrobenzo[b][1,4]dioxine-2-carbonyl)piperazin-1-yl)sulfonyl)pyrimidine-2,4(1H,3H)-dione
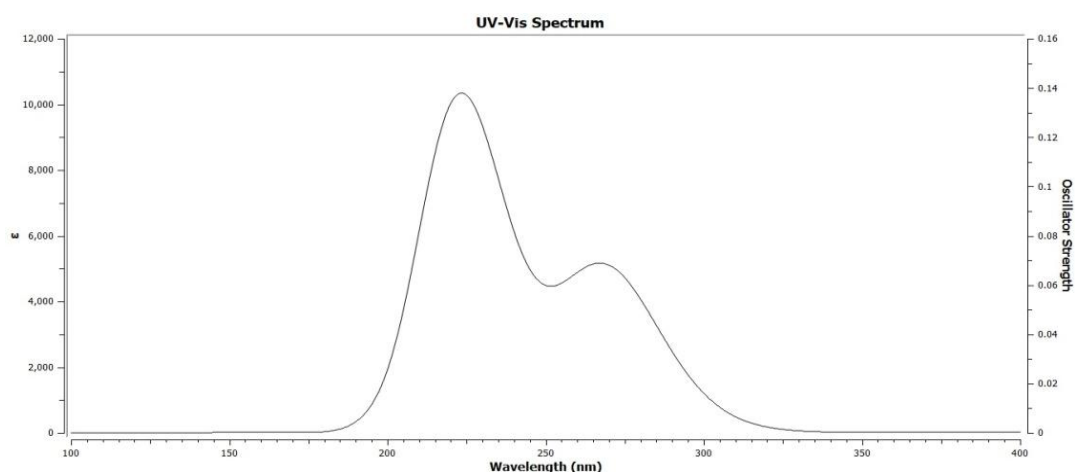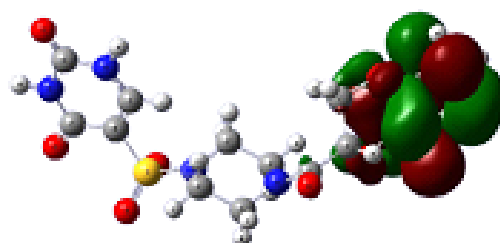

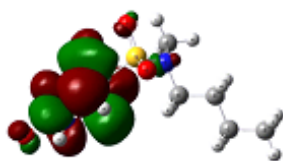**Fig. 12. Computational UV-Vis spectra of N-butyl-N-methyl-2, 4-dioxo-1, 2, 3, 4-tetrahydropyrimidine-5-sulfonamide**

$\Delta E = 0.16719$

Fig. 13. Frontier molecular orbitals of 5-(4-(2,3-dihydrobenzo[b][1,4] dioxine-2-carbonti) piperazin-1-yi) sulfonyi) pyrimidine-2,4(1H,3H)-dione

LUMO

$\Delta E = 0.18998$

Fig.14. Frontier molecular orbitals of N-butyi-N-methyi-2, 4-dioxo-1, 2, 3, 4-te trah ydropyrimidine-5-sulfonamide

Table 1. Machine learning tool to predict the pharmacokinetic properties (ADMET)

pk CSM (ADMET)	Compound-I	Compound-II
Water solubility	-2.958	-2.817
Caco2 permeability	0.669	-0.036
Intestinal absorption (human)	68.255	61.512
BBB permeability	-1.021	-0.525
CNS permeability	-3.338	-3.209
AMES toxicity	No	No
Max. tolerated dose (human)	0.284	1.082
Oral Rat Acute Toxicity (LD50)	1.758	1.799
Oral Rat Chronic Toxicity (LOAEL)	2.354	2.052
T.Pyriformis toxicity	0.287	0.077
LogP	-1.2639	-0.5162

Table 2. "Swiss ADME" a web tool used to predict physicochemical properties, pharmacokinetics, Lipophilicity and drug-likeness

Properties	Compound-I	Compound-II
iLOGP	1.85	0.85
XLOGP3	-0.87	-0.36
WLOGP	-0.94	0.56
MLOGP	-0.83	-0.53
ESOL Class	Very soluble	Very soluble
Ali Class	-1.8	-1.52
GI absorption	Low	High
log Kp (cm/s)	-9.49	-8.15
Lipinski #violations	1	0
Ghose #violations	1	0
Veber #violations	1	0
Egan #violations	1	0
Muegge #violations	1	0
Bioavailability Score	0.55	0.55

Table 3. Chemaxon used to predict logP values

Properties	Compound-I	Compound-II
Lipinski's rule of five	TRUE	TRUE
Topological polar surface area	134.35	95.58
Polarizability	38.72 A3	24.24 A3
Molar refractivity	98.43 cm3/mol	61.78 cm3/mol

4.4 Chem Axon

Chemaxon is used to predict logP values and other structural properties. These parameters have been calculated and are summarized in Table 3.

4.3 Swiss ADME

"SwissADME" a web tool used to predict physicochemical properties, pharmacokinetics, Lipophilicity and drug-likeness among which in-house proficient methods such as the iLOGP and Bioavailability score. These parameters have been calculated and are summarized in Table 2.

5. CONCLUSION

The energies and distributions of the FMO are extremely advantageous indicators of reactivity. The limits of Hyperpolarizability, HOMO and LUMO are listed. The energy gap between the HOMO and LUMO orbital's is a critical parameter in determining and understanding molecular transport properties. Pharmacokinetic properties (ADMET), drug similarity, bioactivity school, logP, pKa calculated using Molinspiration, pkCSM, Swiss ADME, Chem Axon.

DISCLAIMER

The products used for this research are commonly and predominantly use products in our area of research and country. There is absolutely no conflict of interest between the authors and producers of the products because we do not intend to use these products as an avenue for any litigation but for the advancement of knowledge. Also, the research was not funded by the producing company rather it was funded by personal efforts of the authors.

CONSENT

It is not applicable.

ETHICAL APPROVAL

It is not applicable.

COMPETING INTERESTS

Authors have declared that no competing interests exist.

REFERENCES

1. Charles H, Chaudhuri K , Peter D, Mooren D, lois griesbach, Robert D, Schnitzer J, Pleven J, Scheiner. Fluorinated pyrimidines, a new class of tumor-inhibitory compounds. Nature. 1957; 179:663-666.

2. Venkata Sasidhar B. Synthesis and Biological Evaluation of 5-Sulfonamide-Pyrimidine-2,4(1H,3H)-Dione Derivtives as Active Anti-HIV and Anti Cancer Agents, Ph.D. thesis, GITAM (Deemed to be University);2015.

3. Frisch MJ, et al. Pople, Gaussian Inc., Wallingford, CT;2004.

4. Frish A, Nielsen AB, Holder AJ. GAUSSVIEW User Manual, Gaussian Inc., Pittsburg, PA; 2001.

5. Ajmal R Bhat, Rajendra S Dongre, Pervaz A Ganie, Petra, Osiris, Molinspiration: A Computational Bioinformatic Platform for Experimental in vitro Antibacterial Activity of Annulated Uracil Derivatives. Quarterly Journal of Iranian Chemical Communication. 2018;6:114-124.

6. Shefrin S, Asha Asokan Manakadan, Saranya TS. A Computational study of anticancer activity of curcumin derivatives using in silico drug designing and molecular docking tools. Asian Journal of Chemistry. 2018;30:1335-1339.

7. Douglas EV Pires, Tom L Blundell, David B. Ascher, pkCSM: predicting small-molecule pharmacokinetic properties using graph-based signatures. J. Med. Chem. 2015;58:4066–4072.

8. Antoine Daina, Olivier Michielin, Vincent Zoete1, SwissADME: a free web tool to evaluate pharmacokinetics, druglikeness and medicinal chemistry friendliness of small molecules. Scientific reports-nature, 2017; Article number 42717.

9. Arnott JA, Planey SL. The influence of lipophilicity in drug discovery and design. Expert Opin. Drug Discov. 2012;7:863–875.

10. Kamel Mansouri, Neal F. Cariello , Alexandru Korotcov, Valery Tkachenko, Chris M. Grulke, Catherine S. Sprankle, David Allen, Warren M. Casey, Nicole C. Kleinstreuer, Antony J. Williams. Journal of Cheminformatics;2019.

11. Muthu Sambanthan, Maheswari J. Quantum mechanical study and spectroscopic (FT-IR, FT-Raman, C-13, H-1, UV) study, first order hyperpolarizability, NBO analysis, HOMO and LUMO analysis of 4-[(4-aminobenzene) sulfonyl] aniline by ab initio HF and density functional method. Spectrochimicaacta. Part A, Molecular and

biomolecular spectroscopy. 2012;92:154-63.
DOI:10.1016/j.saa.2012.02.056.

12. Fritzsche, Hartmut. Vibrational spectra of benzene derivatives: Von G. Varsányi. AkadémiaiKiadó, Budapest. 1969, 430 Seiten mitzahlreichen Bildern und Tabellen, Format 16, 5×23 cm, Ln. Zeitschriftfür Chemie;2010.
DOI:10. 10.1002/zfch.19700100626.

13. Pir H, Gunay N, Tamer O, Avcı D, Atalay Y. Theoretical investigation of 5-(2-Acetoxyethyl)-6-methylpyrimidin-2,4-dione: conformational study, NBO and NLO analysis, molecular structure and NMR spectra, Spectrochim. Acta. 2013;Part A 112:331-342.

14. Yadav LDS. Organic Spectroscopy, Anamaya Publishers, New Delhi, India; 2005.

15. Balachandran V, Rajeswari S, Lalitha S. DFT computations, vibrational spectra, monomer, dimer, NBO and NMR analyses of antifungal agent: 3,5-Dibromosalicylic acid, J. Mol. Struct. 2012; 1007:63-73.

16. Bardak F, Karaca C, Bilgili S, Atac A, Mavis T, Asiri AM, Karabacak M, Kose E.

Conformational, electronic, and spectroscopic characterization of isophthalic acid (monomer and dimer structures) experimentally and by DFT, Spectrochim. Acta. 2016; Part A165:33e46.

17. Arivazhagan M, Anitha Rexalin D. Vibrational spectra, UV–vis spectral analysis and HOMO–LUMO studies of 2,4-dichloro-5-nitropyrimidine and 4-methyl-2-(methylthio) pyrimidine, Spectrochimica Acta Part A: Molecular and Biomolecular Spectroscopy. 2013;107:347-358.

18. Sudhir M. Hiremath, Suvitha A, Ninganagouda R. Patil, Chidanandayya, Hiremath S, Seema S. Khemalapure, Subrat K. Pattanayak, Veerabhadrayya, S. Negalurmath, Kotresh Obelannavar, J. Sanja, Stevan Armakovi, Armakovi, Synthesis of 5-(5-methyl-benzofuran-3-ylmethyl)-3H-[1, 3, 4] oxadiazole-2-thione and investigation of its spectroscopic, reactivity, optoelectronic and drug likeness properties by combined computational and experimental approach, Spectrochim. Acta. 2018; Part A 205:95-110.

Peer-review history:
The peer review history for this paper can be accessed here:
https://www.sdiarticle5.com/review-history/78793